

Electronic Supplementary Information (ESI)

Construction of 2,2'-biazulene framework via Brønsted acid-promoted annulation of 2,3-di(1-azulenyl)benzofurans

Taku Shoji,* Naoko Sakata, Yukino Ariga, Akari Yamazaki, Ryuzi Katoh, Tetsuo Okujima,
Ryuta Sekiguchi, and Shunji Ito

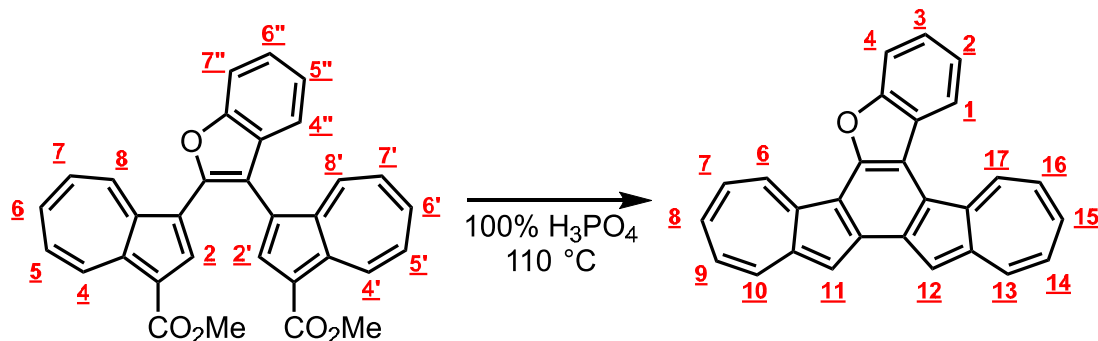
➤ **Contents**

1. Experimental detail	S1–S4
2. Copies of ^1H NMR, ^{13}C NMR, COSY and HRMS (Figures S1–S15).	S5–S12
3. Frontier Kohn–Sham orbitals of 2a–2c (Figures S16–S18).	S13–S16
4. Fluorescence decay profile of 2a–2c (Figures S19–S21).	S17–S18
5. Scope and limitation.	S19–S20

General: Melting points were determined with a Yanagimoto MPS3 micro melting apparatus and were uncorrected. High-resolution mass spectra were obtained with a JEOL JMS-700 spectrometer. UV/Vis spectra were measured with a Shimadzu UV-2550 or a JASCO V-770 spectrophotometers. The fluorescence quantum yield was obtained with an absolute photoluminescence quantum yield spectrometer (Hamamatsu, C11347). The fluorescence lifetime was obtained with a time-resolved fluorescence spectrometer based on a streak camera (Hamamatsu, C4334). Time resolution was about 500 ps. The excitation wavelength was 400 nm (second harmonic of the output from a Ti:sapphire laser; Spectra-Physics, Tsunami). The repetition rate of the oscillator was reduced from 80 to 8 MHz with a pulse selector (Spectra-Physics, Model 3980). ^1H and ^{13}C NMR spectra were recorded with a JEOL ECA500 at 500 MHz (^1H NMR) and 125 MHz (^{13}C NMR), or a JEOL ECZ400 at 400 MHz (^1H NMR) and 100 MHz (^{13}C NMR), respectively.

1. Experimental details

Compound 2a

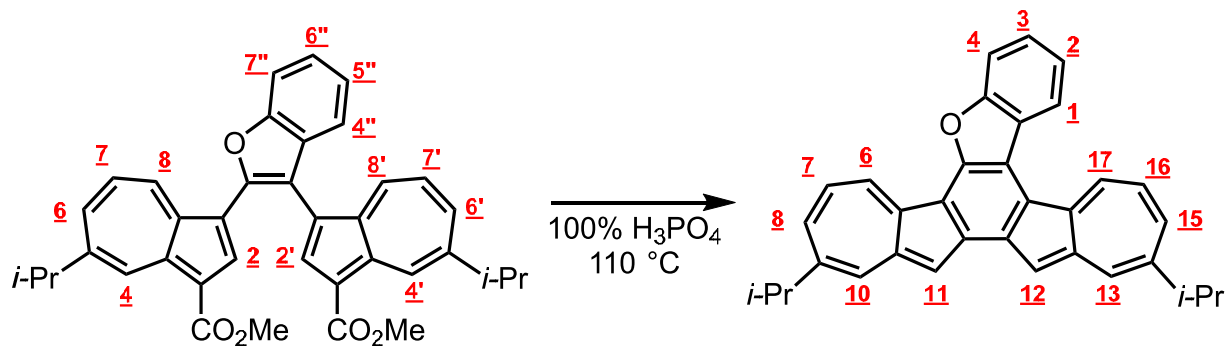


A solution of **1a** (133 mg, 0.273 mmol) in 100% H_3PO_4 (10 mL) was stirred at 110 °C for 1 hour.

After the reaction mixture was cooled, it was poured into water. The generated precipitate was corrected by filtration and washed with methanol to give **2a** (78 mg, 77%) as brown solid.

M.p. > 300 °C; ^1H NMR (500 MHz, 10% $\text{CF}_3\text{CO}_2\text{D}/\text{CDCl}_3$): $\delta_{\text{H}} = 10.45$ (d, $J = 10.1$ Hz, 1H, H_6 or H_{17}), 10.38 (d, $J = 10.1$ Hz, 1H, H_6 or H_{17}), 9.44-9.40 (m, 2H, $\text{H}_{10,13}$), 9.36-9.28 (m, 2H, $\text{H}_{7,16}$), 9.08 (m, 4H, $\text{H}_{8,9,14,15}$), 8.61 (d, $J = 8.1$ Hz, 1H, H_2 or H_3), 8.05 (d, $J = 8.1$ Hz, 1H, H_2 or H_3), 7.89 (t, $J = 8.1$ Hz, 1H, H_1 or H_4), 7.74 (t, $J = 8.1$ Hz, 1H, H_1 or H_4) ppm, The protons H_{11} and H_{12} were disappeared by the proton-deuterium exchange in 10% $\text{CF}_3\text{CO}_2\text{D}/\text{CDCl}_3$ mixed solvent; measurement of ^{13}C NMR was hampered by the low solubility of compound; HRMS (MALDI-TOF, positive): $\text{C}_{28}\text{H}_{16}\text{O}^+ [\text{M}]^+$ calcd:368.1196; found:368.1192.

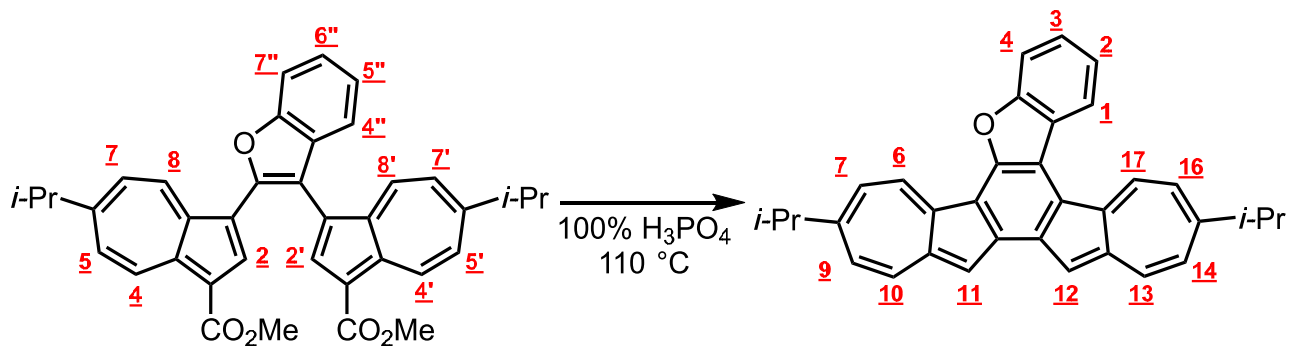
Compound 2b



A solution of **1b** (99 mg, 0.195 mmol) in 100% H_3PO_4 (10 mL) was stirred at 110 °C for 1 hour. After the reaction mixture was cooled, it was poured into water and extracted with CHCl_3 . The crude product was purified by silica gel column chromatography with CHCl_3 as the eluent to afford **2b** (66 mg, 75%) as brown solid.

M.p. > 300 °C; ^1H NMR (500 MHz, CDCl_3): $\delta_{\text{H}} = 9.47$ (d, $J = 9.1$ Hz, 1H, H_6 or H_{17}), 9.42 (d, $J = 8.7$ Hz, 1H, H_6 or H_{17}), 8.71-8.73 (m, 1H, H_1), 8.38 (s, 2H, $\text{H}_{10,13}$), 8.04 (s, 1H, H_{11} or H_{12}), 7.96 (s, 1H, H_{11} or H_{12}), 7.86-7.88 (m, 1H, H_4), 7.51-7.58 (m, 4H, $\text{H}_{2,3,8,15}$), 7.44 (dd, $J = 11.0, 8.7$ Hz, 1H, H_7 or H_{16}), 7.36 (dd, $J = 10.9, 9.1$ Hz, 1H, H_7 or H_{16}), 3.18–3.11 (m, 2H, *i*-Pr), 1.45 (d, $J = 6.9$ Hz, 12H, *i*-Pr) ppm; ^{13}C NMR (125 MHz, CDCl_3): $\delta_{\text{C}} = 156.15, 151.18, 143.36, 141.70, 139.87, 138.45, 137.90, 137.44, 137.09, 135.07, 134.86, 134.69, 134.49, 132.92, 125.27, 124.83, 124.09, 122.85, 122.55, 115.34, 114.26, 113.90, 112.90, 111.91, 38.71, 38.41, 24.49$ ppm, signals of *i*-Pr is overlapped; HRMS (MALDI-TOF, positive): $\text{C}_{34}\text{H}_{28}\text{O}^+ [\text{M}]^+$ calcd: 452.2135; found: 452.2147.

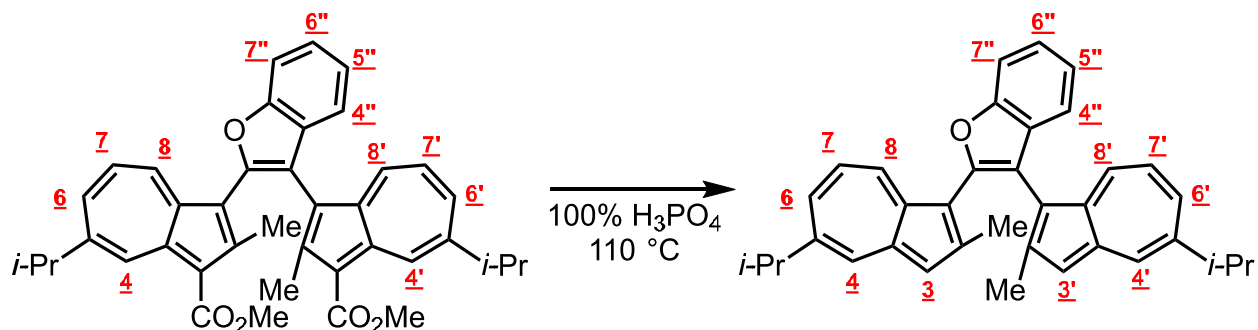
Compound 2c



A solution of **1c** (121 mg, 0.212 mmol) in 100% H₃PO₄ (10 mL) was stirred at 110 °C for 1 hour. After the reaction mixture was cooled, it was poured into water and extracted with CHCl₃. The crude product was purified by silica gel column chromatography with CHCl₃ as the eluent to afford **2c** (71 mg, 74%) as brown solid.

M.p. > 300 °C; ¹H NMR (500 MHz, CDCl₃): δ_H = 9.53 (d, *J* = 9.5 Hz, 1H, H₆ or H₁₇), 9.49 (d, *J* = 9.2 Hz, 1H, H₆ or H₁₇), 8.75-8.77 (m, 1H, H₁), 8.41 (d, *J* = 10.9 Hz, 2H, H₁₀ or H₁₃), 8.10 (s, 1H, H₁₁ or H₁₂), 8.02 (s, 1H, H₁₁ or H₁₂), 7.87-7.89 (m, 1H, H₄), 7.52-7.54 (m, 2H, H_{2,3}), 7.42 (d, *J* = 9.2 Hz, 1H, H₇ or H₁₆), 7.34 (d, *J* = 9.5 Hz, 1H, H₇ or H₁₆), 7.18 (d, *J* = 10.9 Hz, 1H, H₉ or H₁₄), 7.10 (d, *J* = 10.6 Hz, 1H, H₉ or H₁₄), 3.12-3.17 (m, 2H, *i*-Pr), 1.45-1.42 (m, 12H, *i*-Pr) ppm; ¹³C NMR (125 MHz, CDCl₃): δ_C = 158.52, 158.47, 156.19, 151.34, 139.33, 137.41, 137.04, 136.85, 136.66, 136.50, 135.53, 135.37, 134.65, 133.88, 125.33, 124.82, 124.49, 124.41, 123.18, 122.85, 122.64, 120.71, 115.72, 114.73, 114.24, 113.01, 111.92, 77.36, 77.10, 76.85, 39.88, 39.75, 24.29, 24.26 ppm; HRMS (MALDI-TOF, positive): C₃₄H₂₈O⁺ [M]⁺ calcd: 452.2135; found: 452.2113.

Compound 3



A solution of **1d** (115 mg, 0.192 mmol) in 100% H_3PO_4 (10 mL) was stirred at 110 °C for 1 hour. After the reaction mixture was cooled, it was poured into water and extracted with toluene. The crude product was purified by silica gel column chromatography with toluene as the eluent to afford **3** (88 mg, 95%) as blue solid.

M.p. 103–105 °C; ^1H NMR (500 MHz, CDCl_3): $\delta_{\text{H}} = 8.24$ (d, $J = 9.7$ Hz, 1H, $\text{H}_{8'} \text{ or } \text{H}_{8''}$), 8.11 (s, 1H, $\text{H}_{4'} \text{ or } \text{H}_{4''}$), 8.09 (d, $J = 1.1$ Hz, 1H, $\text{H}_{4'} \text{ or } \text{H}_{4''}$), 8.07 (d, $J = 9.7$ Hz, 1H, $\text{H}_{8'} \text{ or } \text{H}_{8''}$), 7.65 (d, $J = 7.7$ Hz, 1H, H_4), 7.33-7.43 (m, 4H, $\text{H}_{5,7,6',6''}$), 7.22 (t, $J = 7.4$ Hz, 1H, H_6), 7.06 (s, 1H, $\text{H}_{3'} \text{ or } \text{H}_{3''}$), 7.00 (s, 1H, $\text{H}_{3'} \text{ or } \text{H}_{3''}$), 6.92-6.98 (m, 2H, $\text{H}_{7',7''}$), 3.10–3.01 (m, 2H, *i*-Pr), 2.10 (s, 3H, Me), 2.00 (s, 3H, Me), 1.37 (d, $J = 6.9$ Hz, 6H, *i*-Pr), 1.33 (d, $J = 6.9$ Hz, 6H, *i*-Pr) ppm; ^{13}C NMR (125 MHz, CDCl_3): $\delta_{\text{C}} = 155.15$, 150.88, 150.39, 149.83, 144.53, 143.28, 141.48, 140.89, 138.14, 137.20, 135.40, 134.72, 134.47, 133.92, 132.84, 132.33, 131.09, 124.07, 123.63, 122.51, 122.37, 121.05, 119.73, 118.14, 117.95, 117.53, 113.53, 111.17, 38.57, 38.53, 24.66, 24.57, 15.84, 15.50 ppm; HRMS (MALDI-TOF, positive): $\text{C}_{36}\text{H}_{34}\text{O}^+ [\text{M}]^+$ calcd: 482.2604; found: 482.2620; $\text{C}_{36}\text{H}_{34}\text{O} + \text{Ag}^+ [\text{M} + \text{Ag}]^+$ calcd: 589.1655; found: 589.1663.

2. Copies of ^1H NMR, ^{13}C NMR, COSY and HRMS of reported compounds (Figures S1–S15).

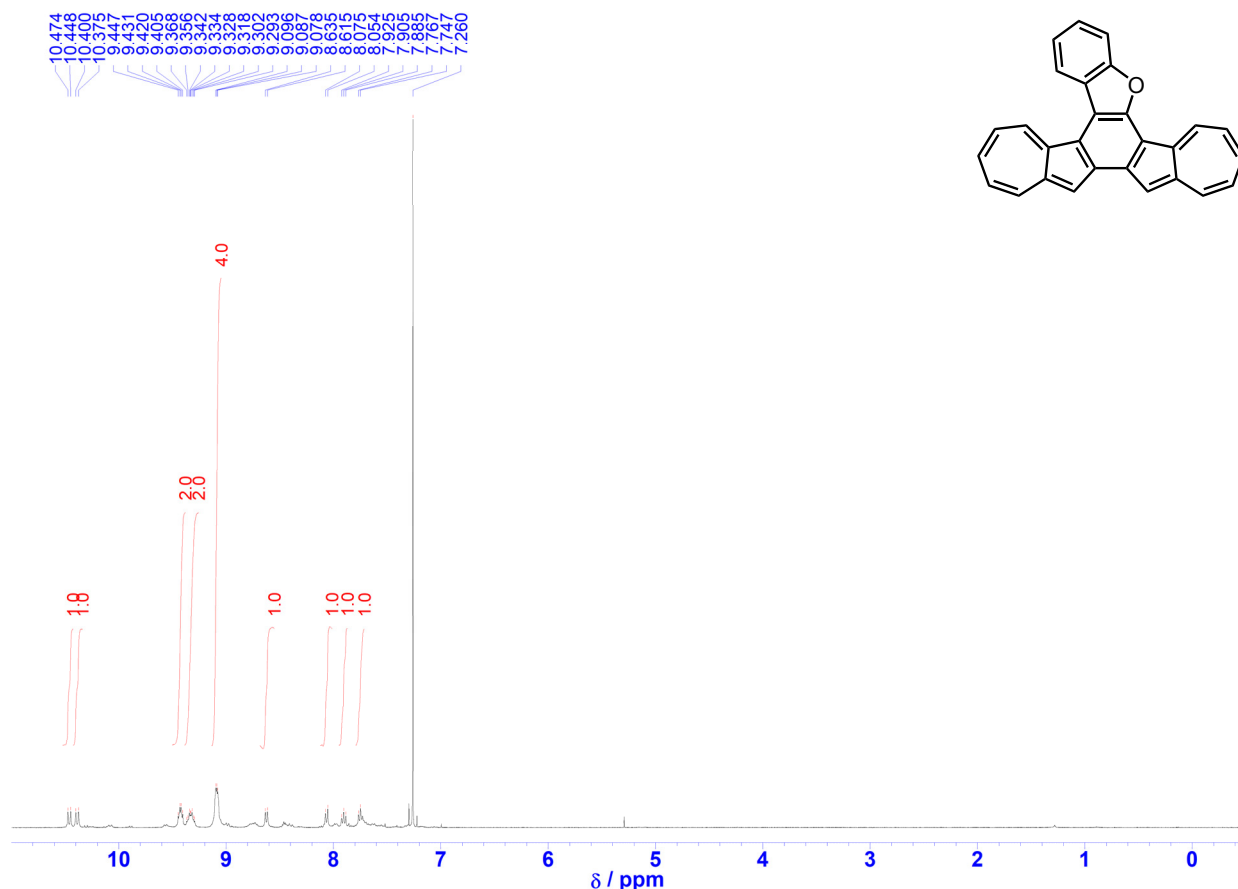


Figure S1. ^1H NMR spectrum of **2a** in 10% $\text{CF}_3\text{CO}_2\text{D}/\text{CDCl}_3$ (400 MHz).

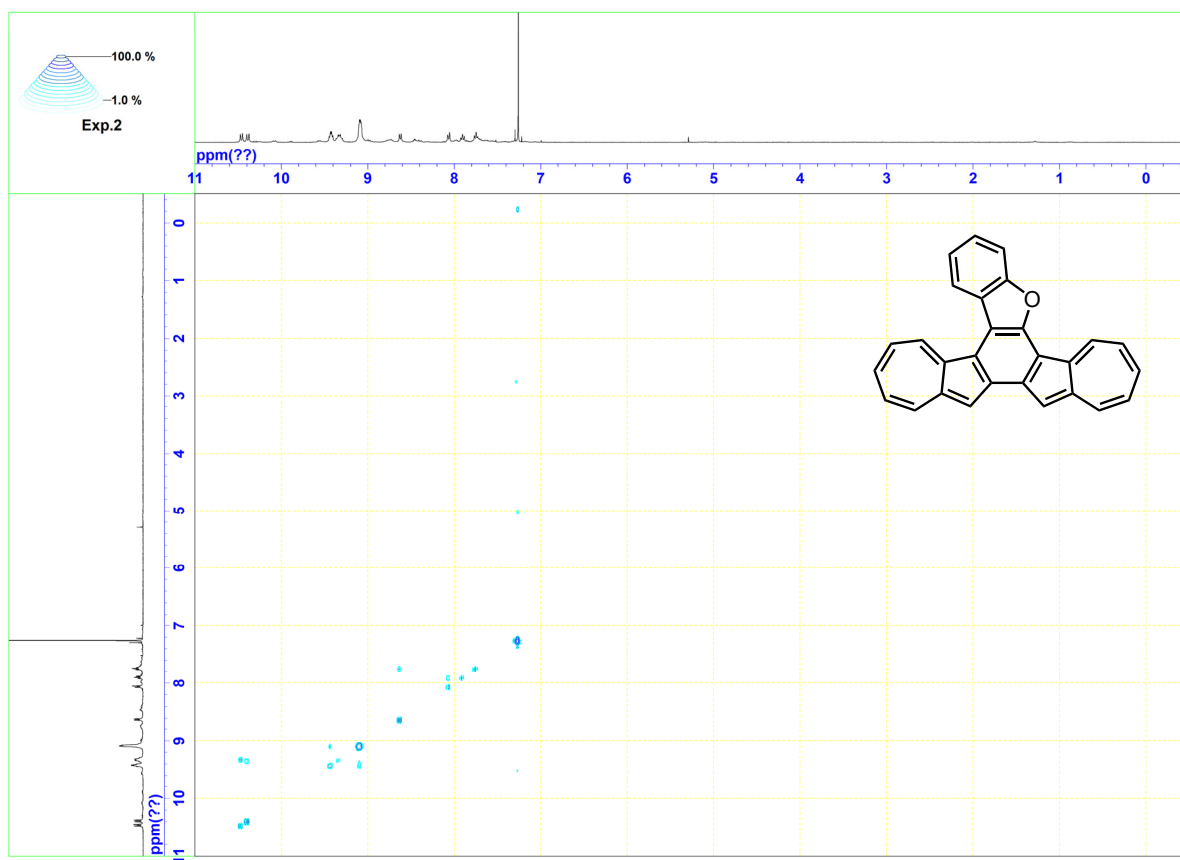


Figure S2. COSY spectrum of **2a** in 10% $\text{CF}_3\text{CO}_2\text{D}/\text{CDCl}_3$ (400 MHz).

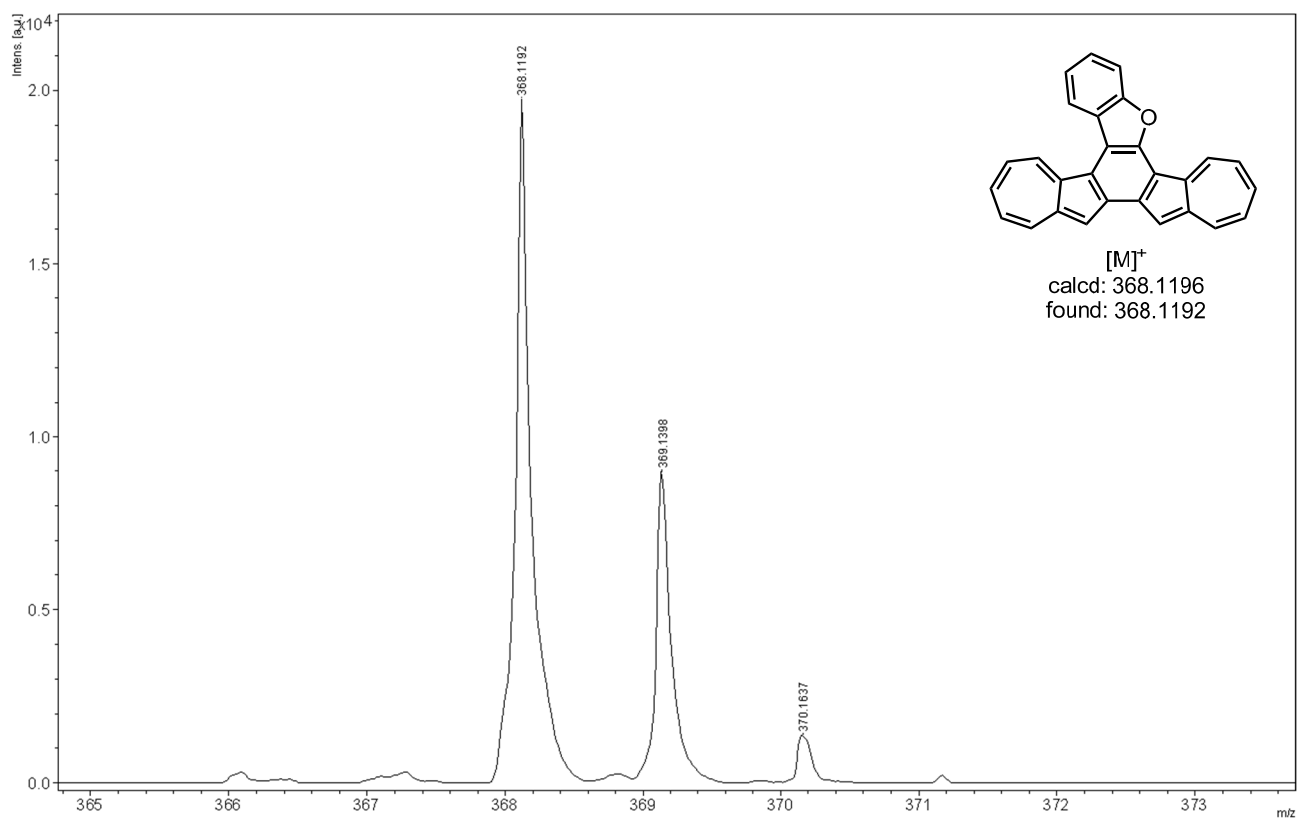


Figure S3. HRMS (MALDI-TOF, positive) of **2a**.



Figure S4. ^1H NMR spectrum of **2b** in CDCl_3 (500 MHz).

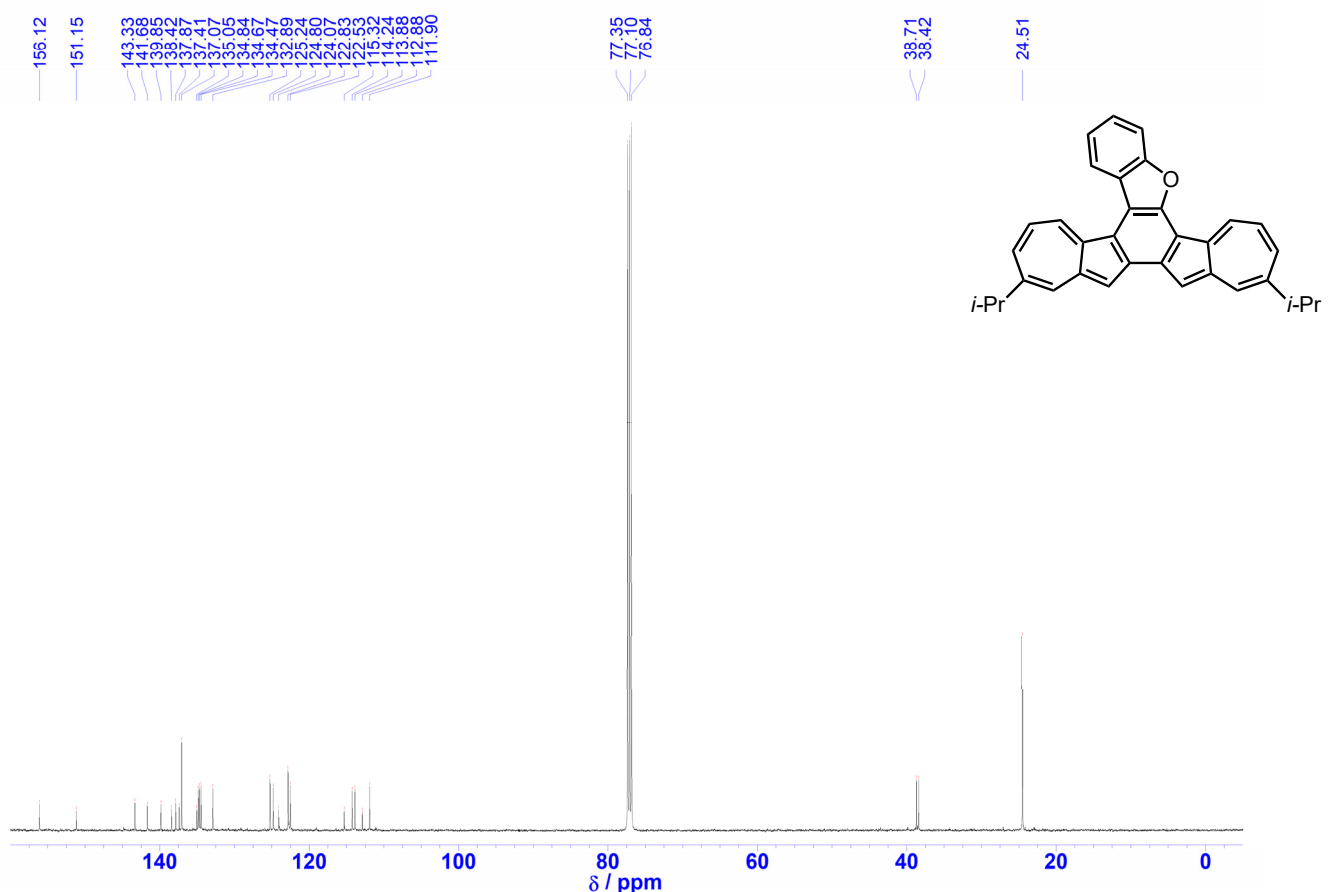


Figure S5. ^{13}C NMR spectrum of **2b** in CDCl_3 (125 MHz).

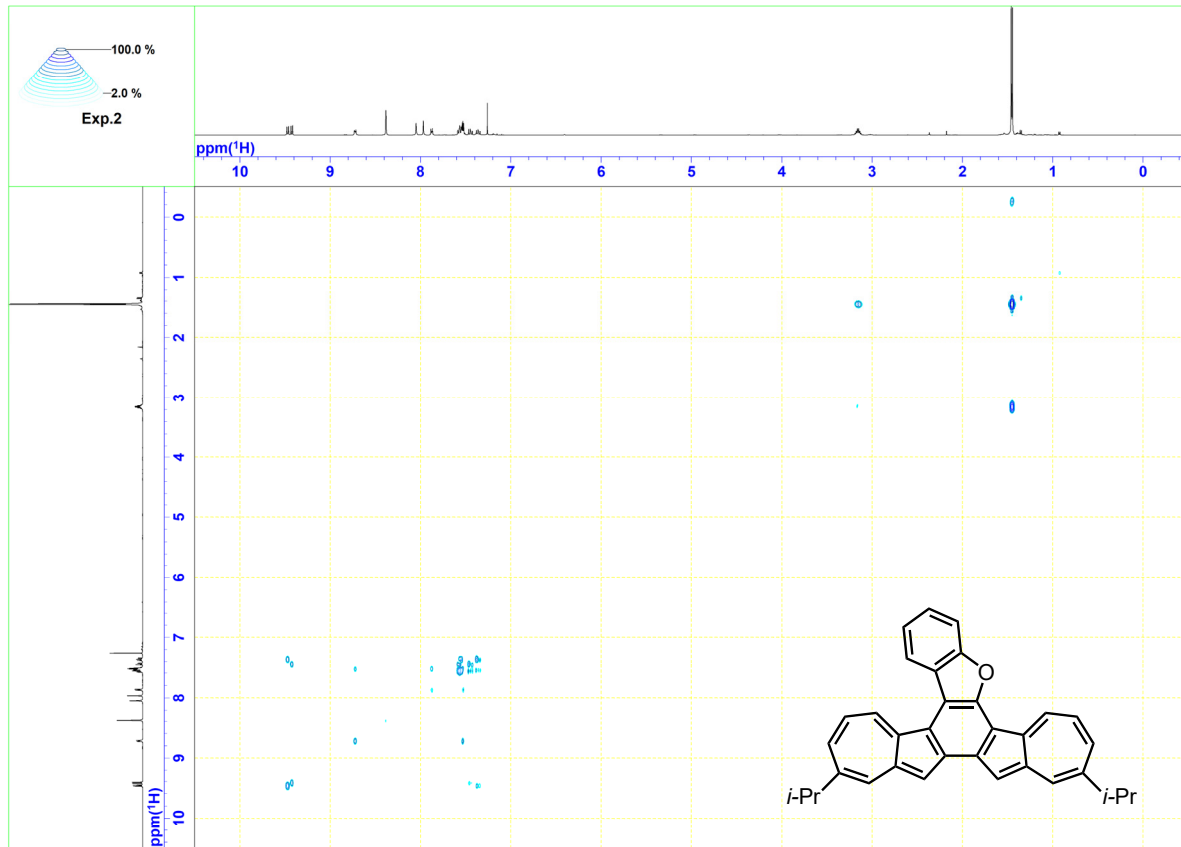


Figure S6. COSY spectrum of **2b** in CDCl₃ (500 MHz).

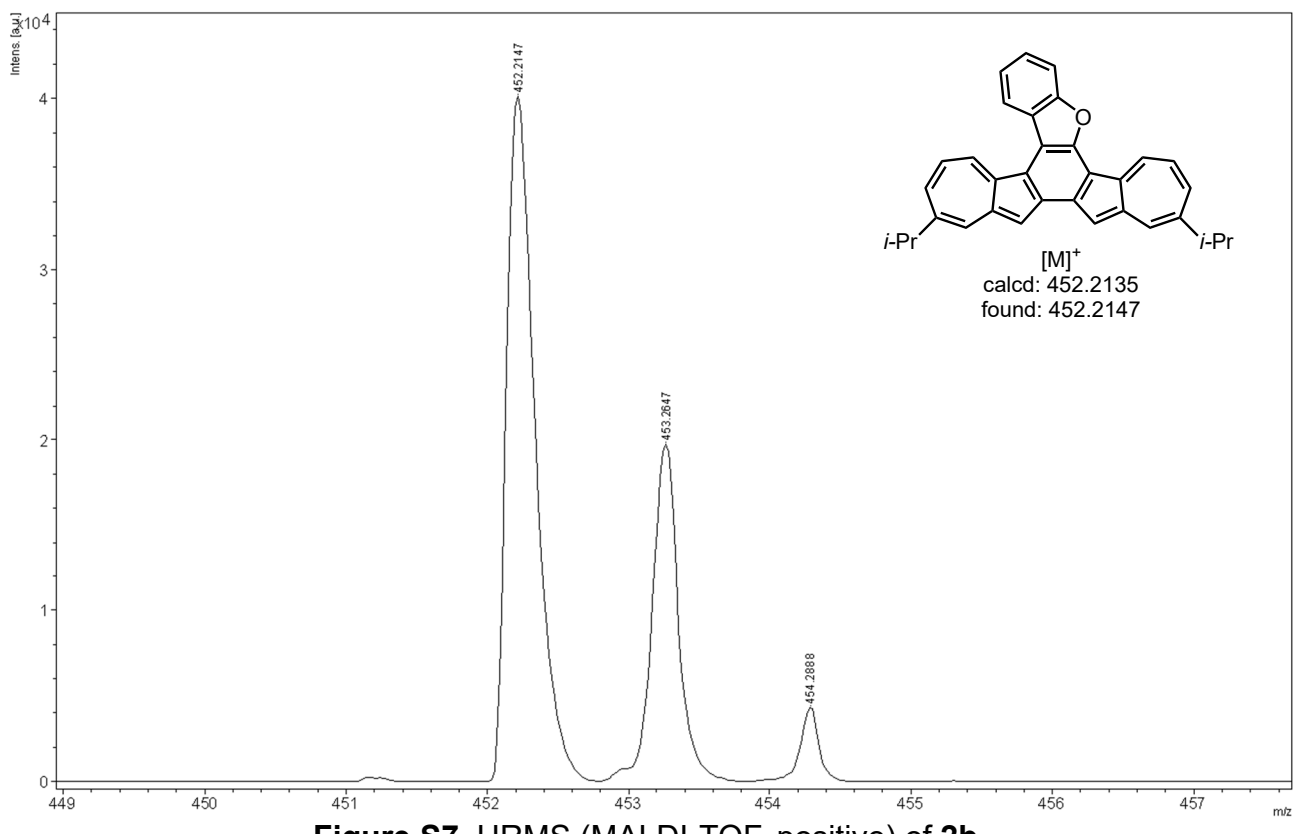


Figure S7. HRMS (MALDI-TOF, positive) of **2b**.

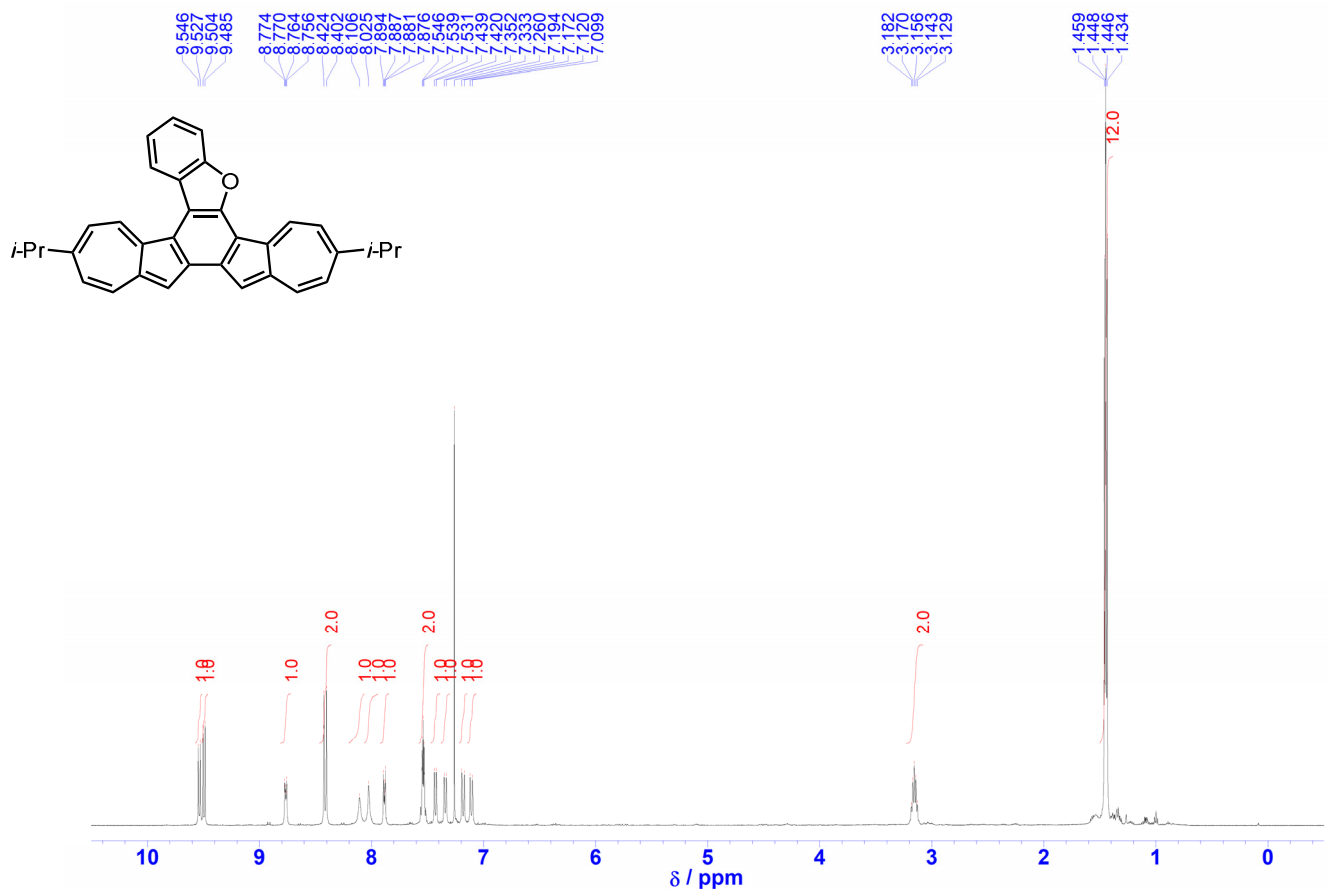


Figure S8. ^1H NMR spectrum of **2c** in CDCl_3 (500 MHz).

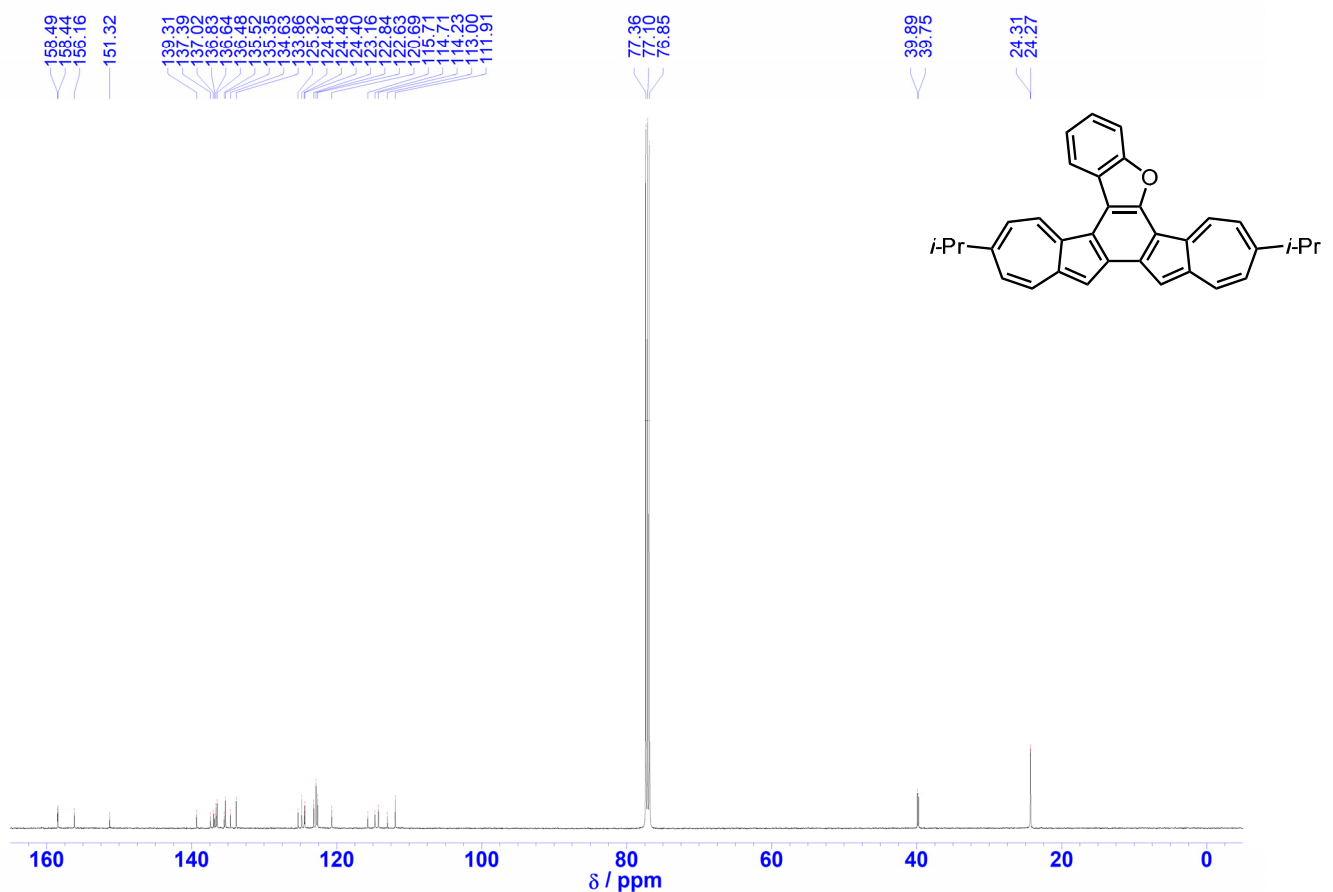


Figure S9. ^{13}C NMR spectrum of **2c** in CDCl_3 (125 MHz).

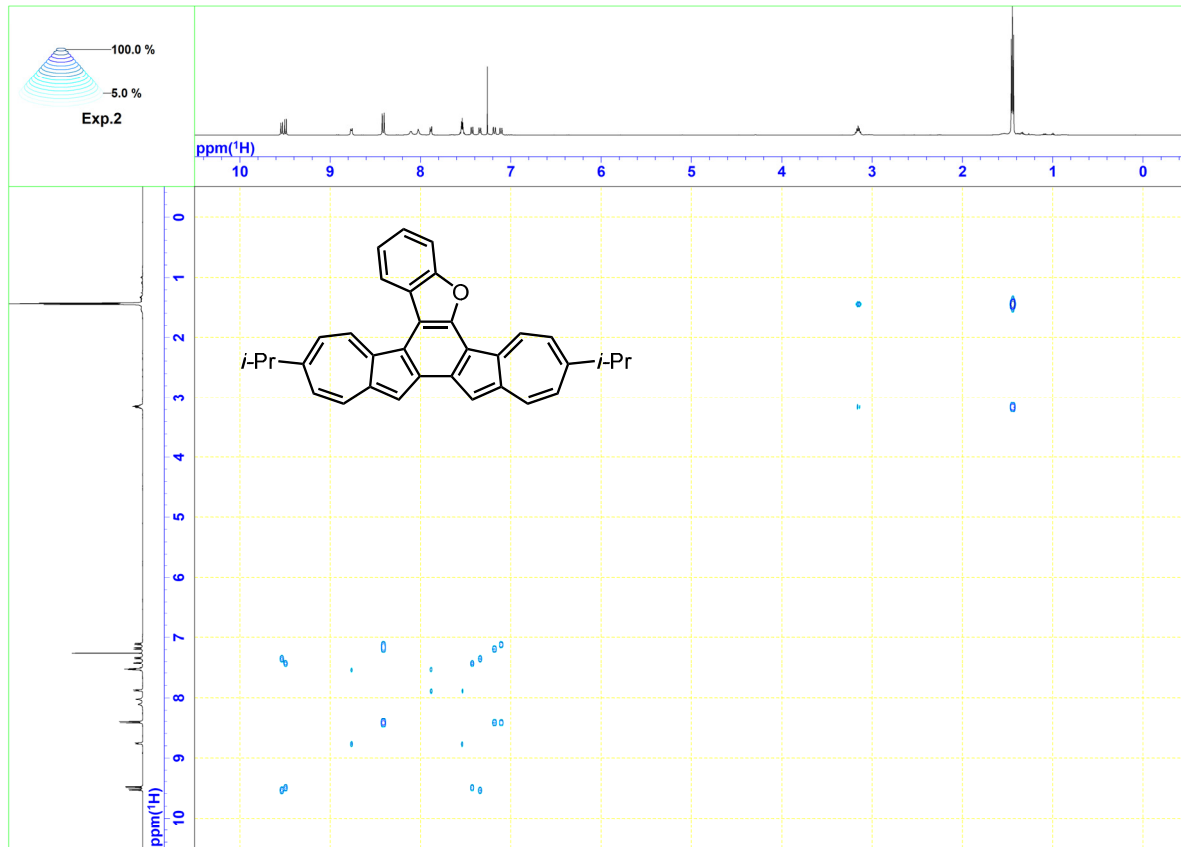


Figure S10. COSY spectrum of **2c** in CDCl_3 (500 MHz).

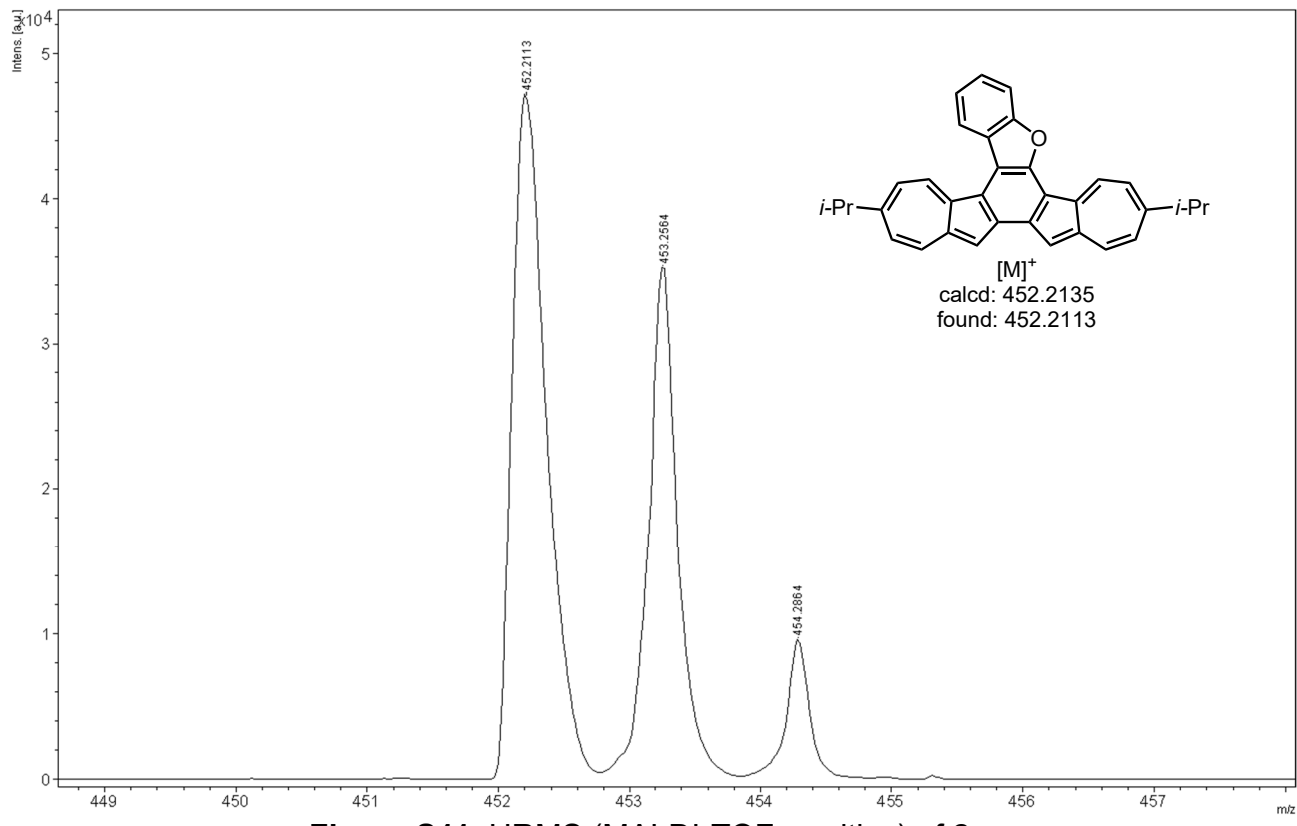


Figure S11. HRMS (MALDI-TOF, positive) of **2c**.

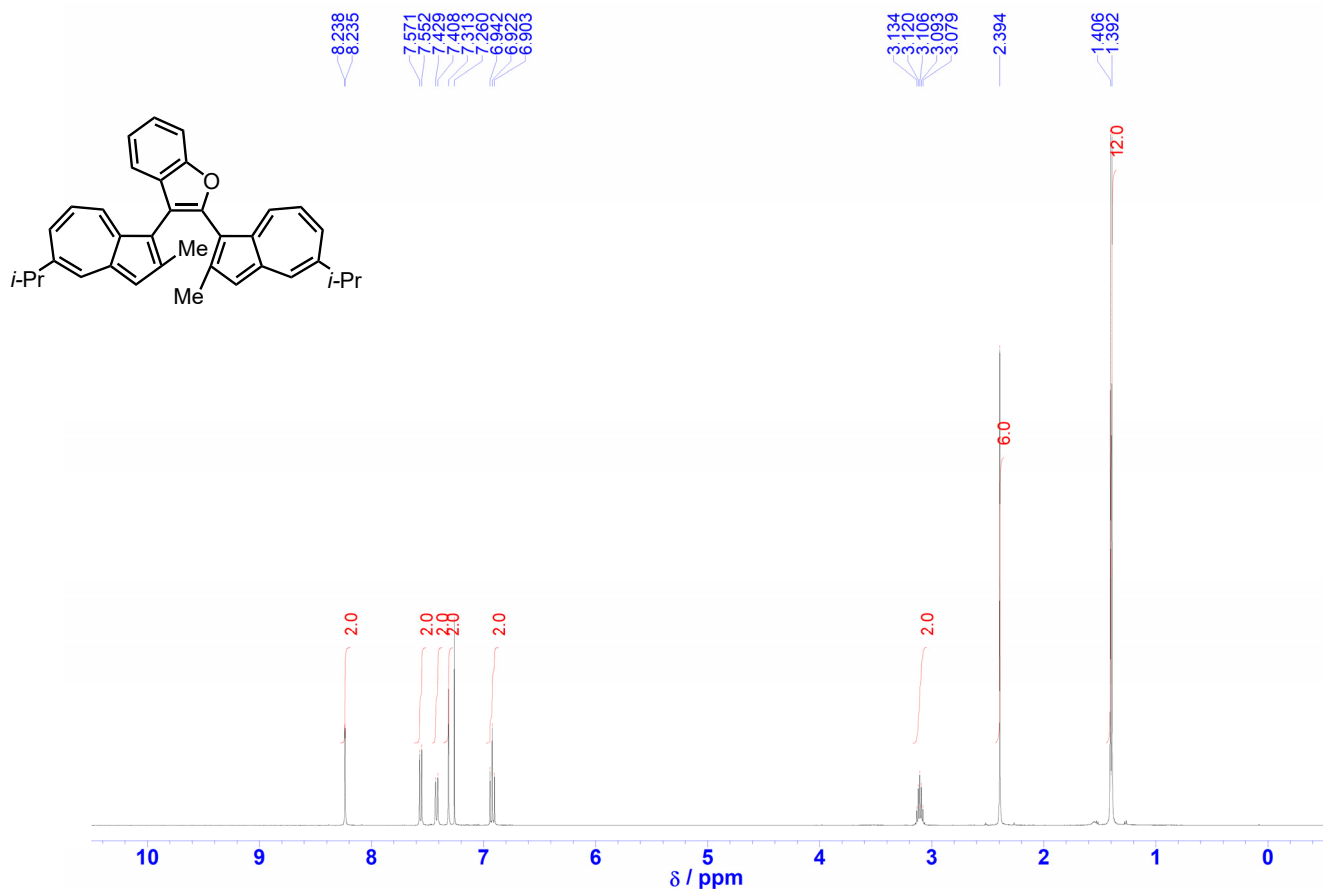


Figure S12. ^1H NMR spectrum of **3** in CDCl_3 (500 MHz).

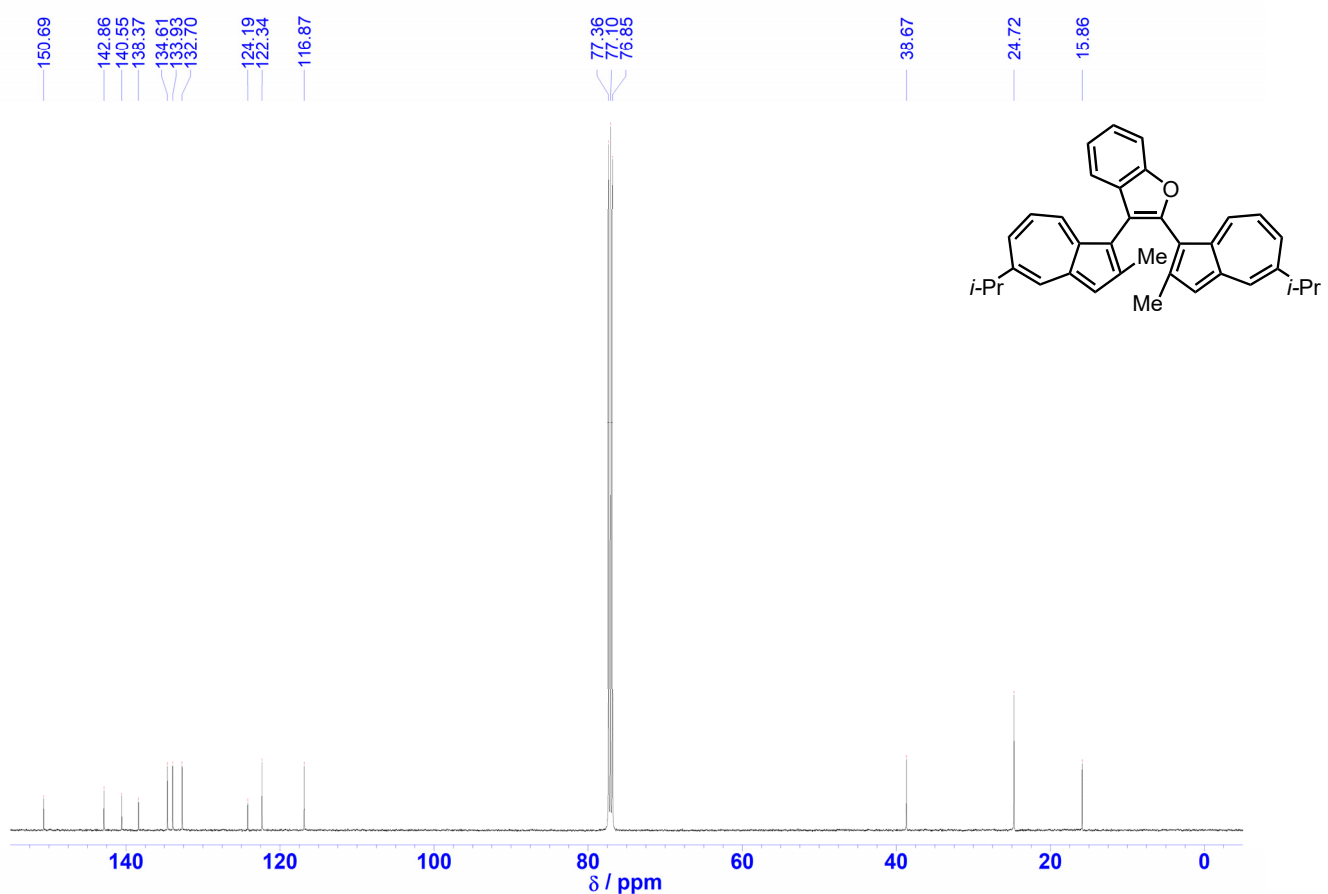


Figure S13. ^{13}C NMR spectrum of **3** in CDCl_3 (125 MHz).

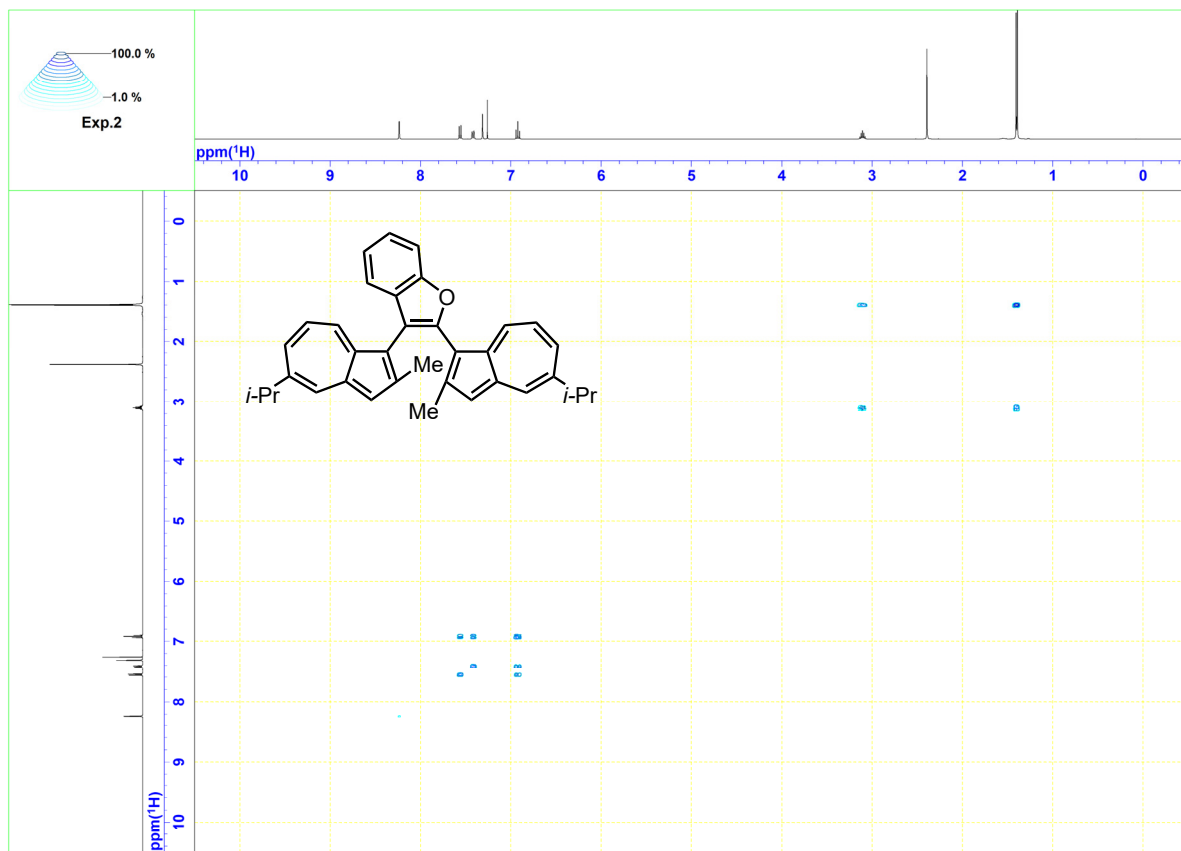


Figure S14. COSY spectrum of **3** in CDCl_3 (500 MHz).

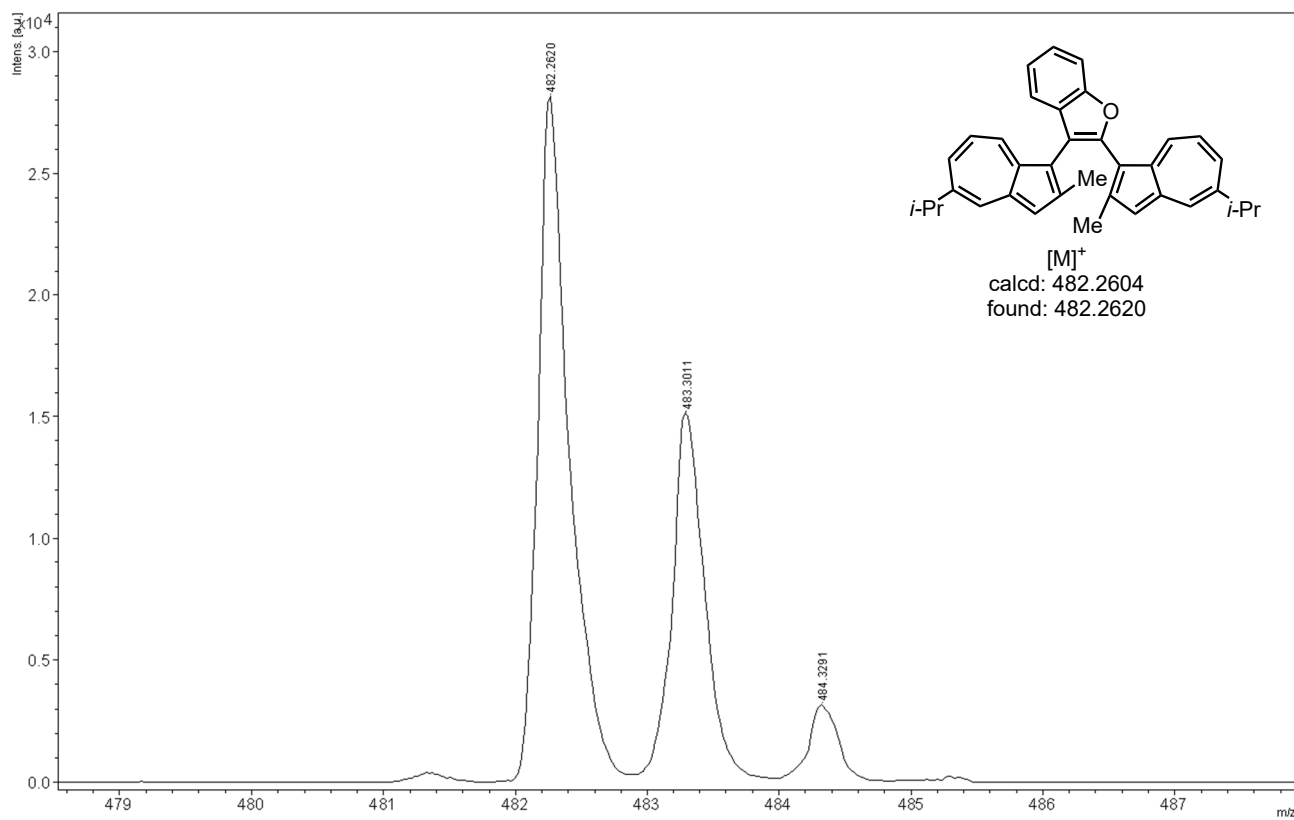
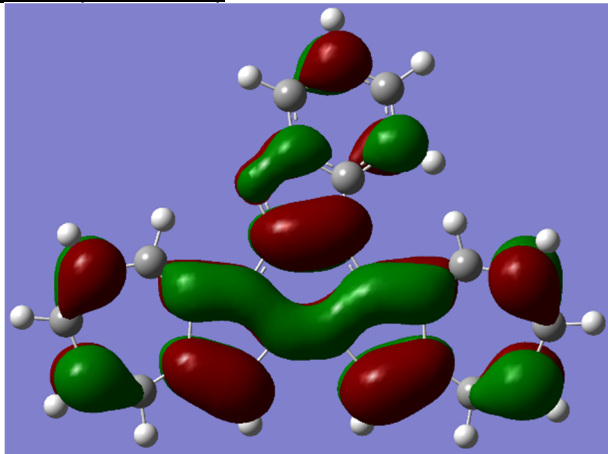


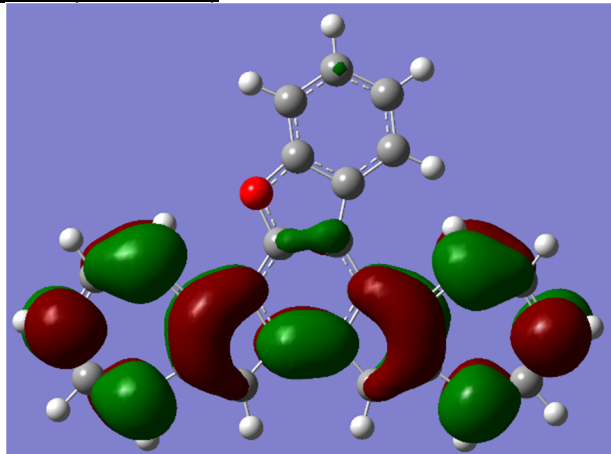
Figure S15. HRMS (MALDI-TOF, positive) of **3**.

3. Frontier Kohn–Sham orbitals of 2a–2c (Figures S16–S18).

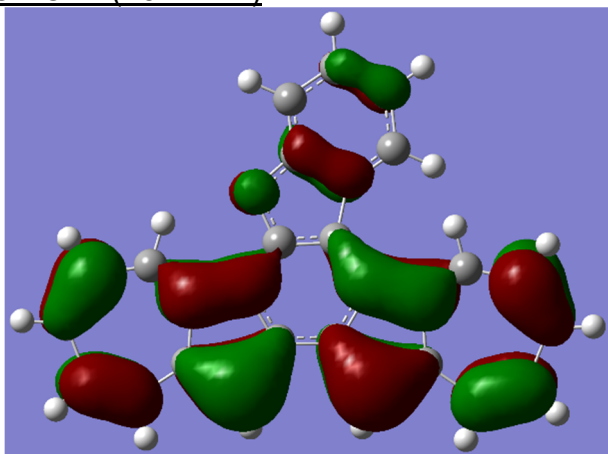
HOMO (-4.52 eV)



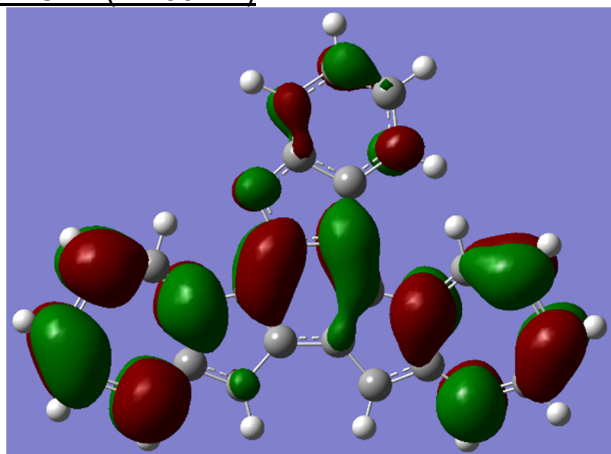
LUMO (-2.37 eV)



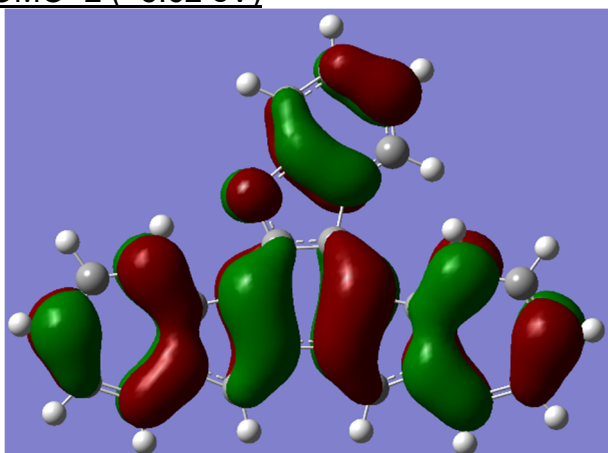
HOMO-1 (-5.44 eV)



LUMO+1 (-1.60 eV)



HOMO-2 (-5.62 eV)



LUMO+2 (-1.33 eV)

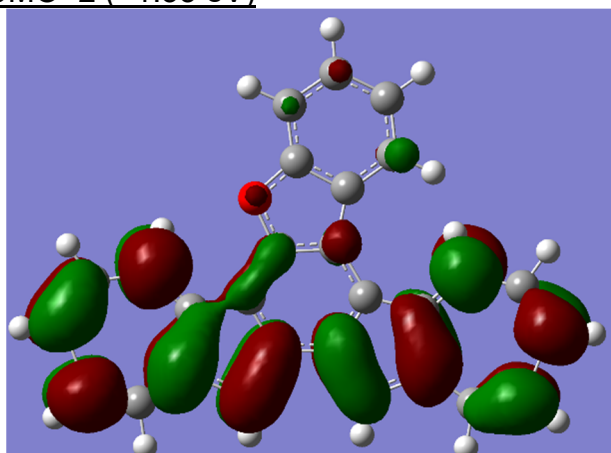
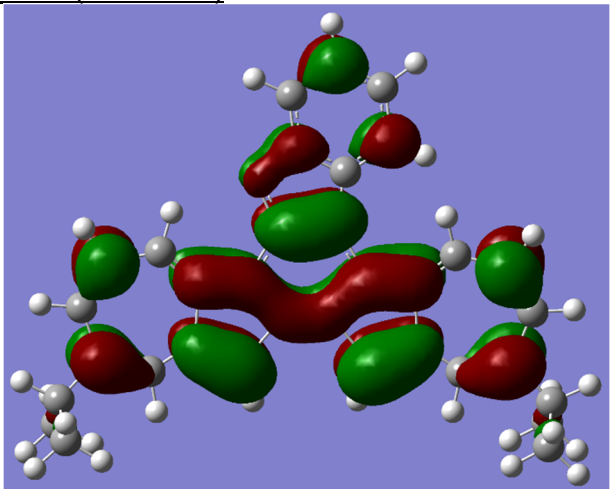
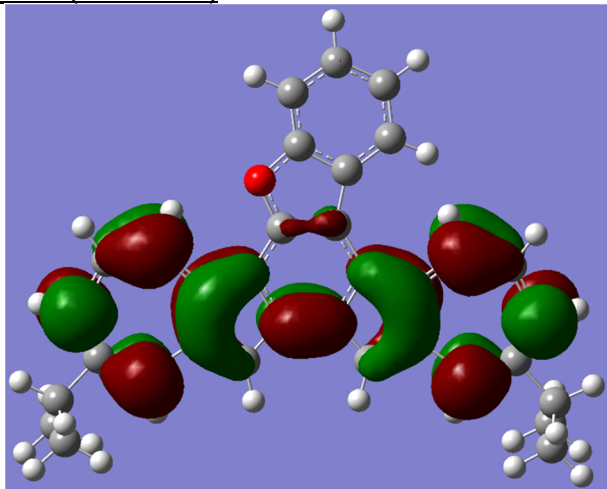


Figure S16. Frontier Kohn–Sham orbitals of **2a** at the B3LYP/6-31G** level.

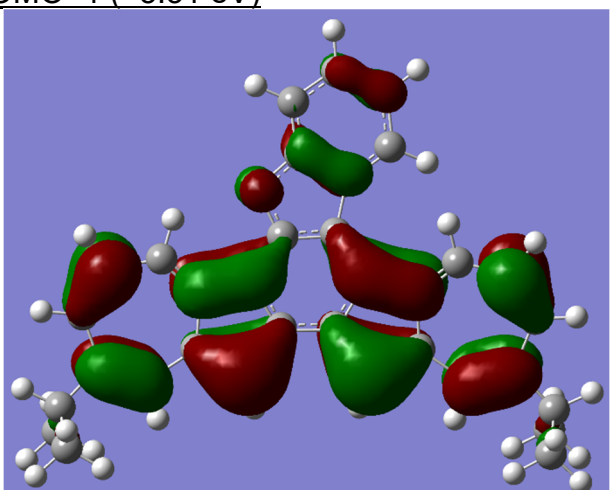
HOMO (-4.38 eV)



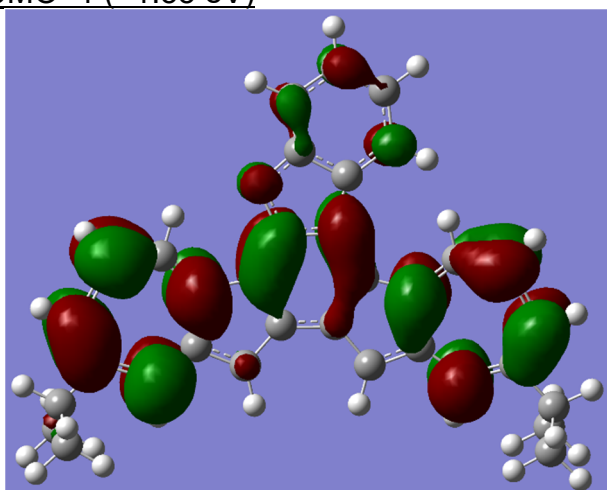
LUMO (-2.30 eV)



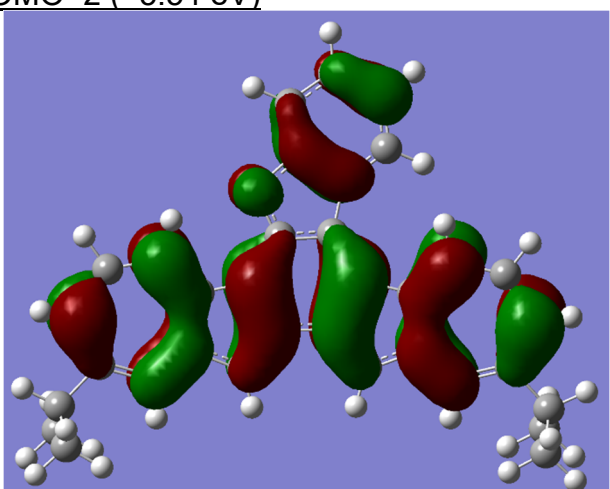
HOMO-1 (-5.31 eV)



LUMO+1 (-1.55 eV)



HOMO-2 (-5.54 eV)



LUMO+2 (-1.24 eV)

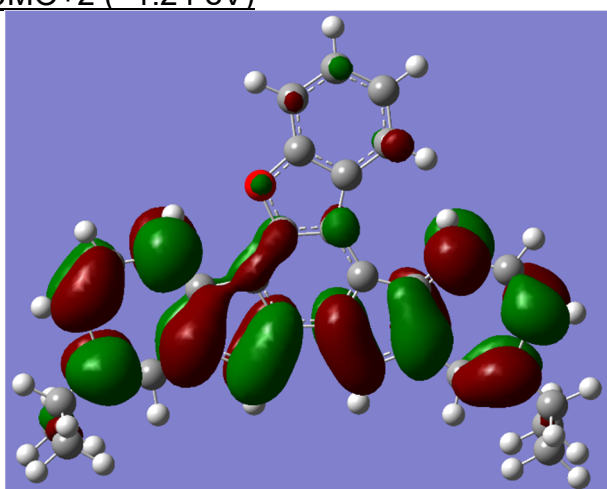
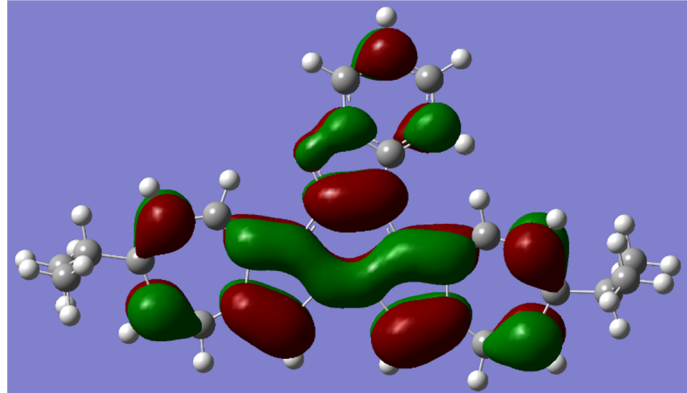
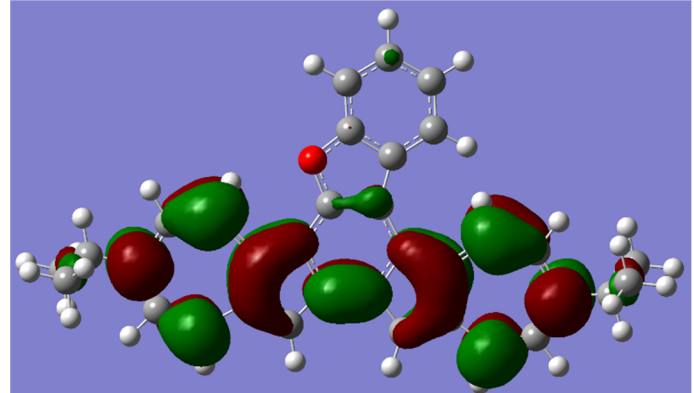


Figure S17. Frontier Kohn–Sham orbitals of **2b** at the B3LYP/6-31G** level.

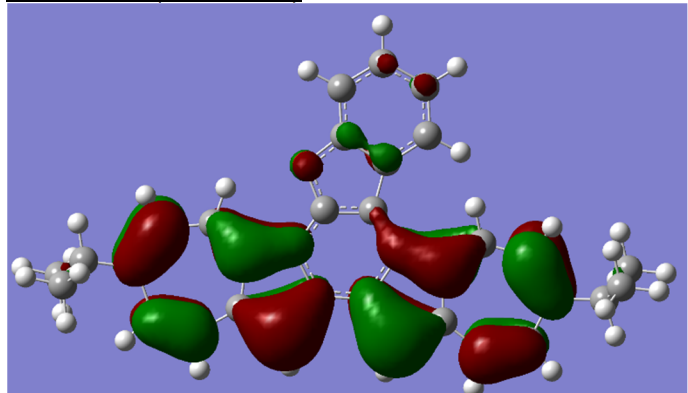
HOMO (-4.41 eV)



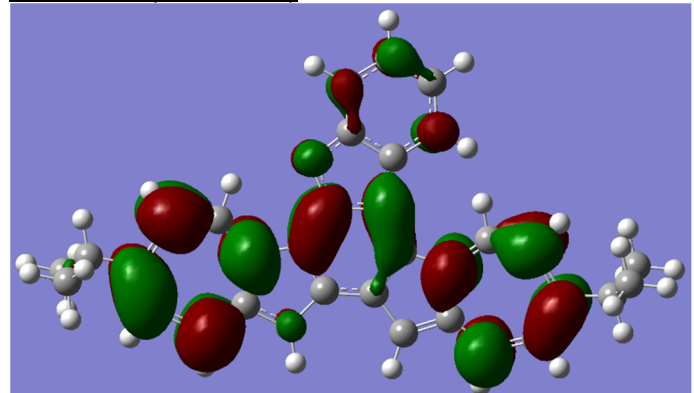
LUMO (-2.23 eV)



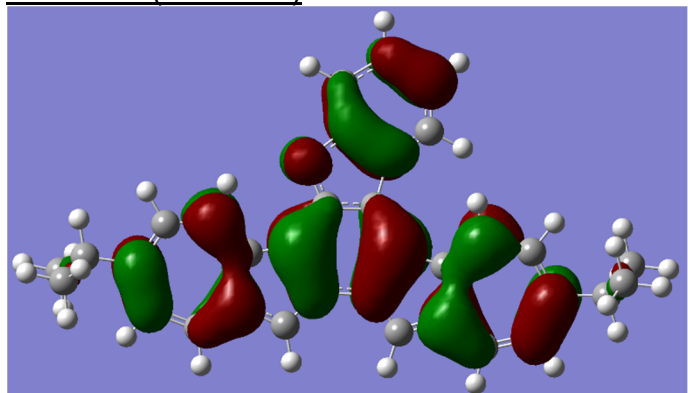
HOMO-1 (-5.32 eV)



LUMO+1 (-1.49 eV)



HOMO-2 (-5.47 eV)



LUMO+2 (-1.23 eV)

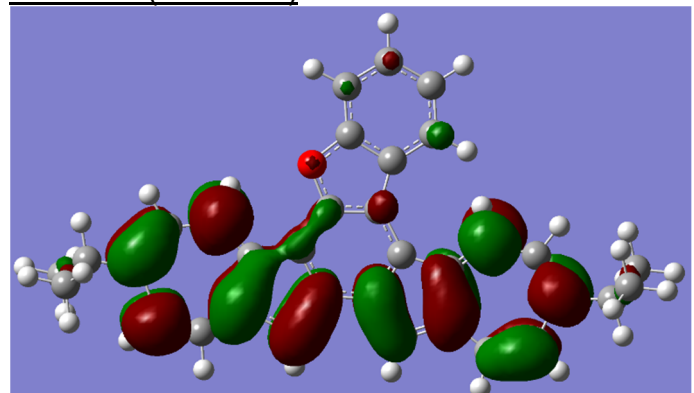


Figure S18. Frontier Kohn–Sham orbitals of **2c** at the B3LYP/6-31G** level.

Table S1. The electronic transitions derived from the computed values based on the TD-DFT calculations at the B3LYP/6-31G** level.

Experimental		Computed Values	
Compound	λ [nm] ($\log \epsilon$)	λ [nm] (Oscillator Strength)	Composition (Contribution, %)
2a	955 (2.67)	829 (0.0155)	H → L (98.2)
	842 (2.82)		
	757 (2.63)		
	581 (2.40)	564 (0.0019)	H-1 → L (30.6)
	537 (2.40)		H → L+1 (56.4)
			H → L+2 (11.5)
	471 (3.86)	493 (0.0316)	H-2 → L (30.7)
			H-1 → L (33.5)
			H → L+1 (30.9)
		479 (0.0011)	H → L+2 (3.9)
2b	979 (2.54)	866 (0.0157)	H → L (98.3)
	860 (2.69)		
	771 (2.48)		
	591 (2.52)	580 (0.0029)	H-1 → L (30.5)
	546 (2.49)		H → L+1 (58.1)
			H → L+2 (10.1)
	491 sh (3.52)	505 (0.00457)	H-2 → L (17.1)
			H-1 → L (51.0)
			H → L+1 (30.5)
	468 (3.87)	483 (0.00457)	H-2 → L (19.3)
2c	911 (2.63)	805 (0.0152)	H → L (98.0)
	808 (2.79)		
	731 (2.58)		
	568 (2.79)	557 (0.0011)	H-1 → L (27.7)
	528 (2.79)		H → L+1 (55.4)
			H → L+2 (13.7)
	472 (3.93)	488 (0.0276)	H-2 → L (48.0)
			H-1 → L (2.0)
			H → L+1 (23.4)
			H-2 → L (25.0)
477 (0.0146)			H-1 → L (54.8)
			H → L+1 (6.2)
			H → L+2 (37.1)

4. Fluorescence decay profile of 2a–2c (Figures S19–S21).

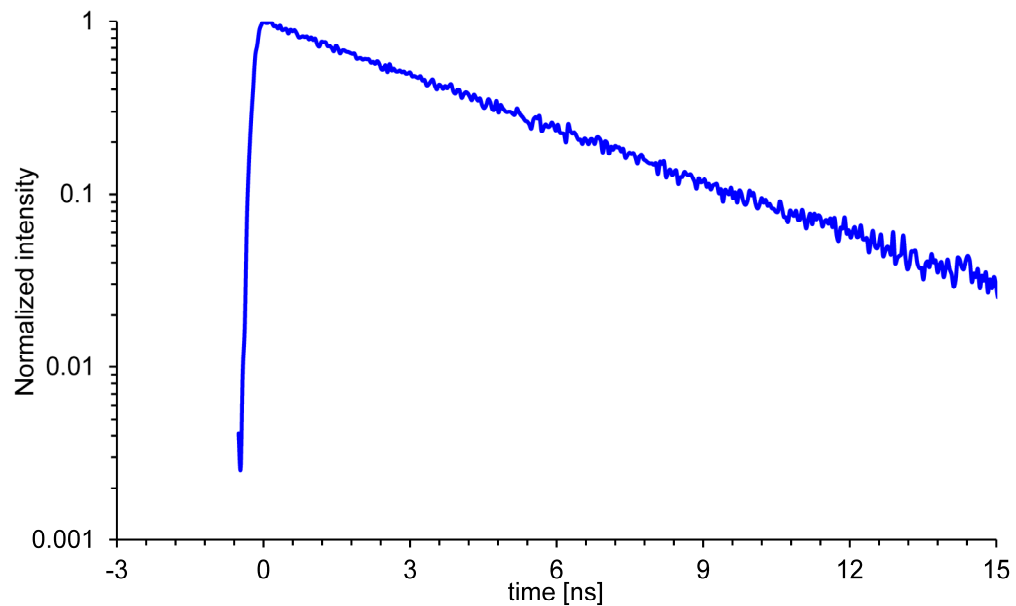


Figure S19. Fluorescence decay profile of **2a** in 10% CF₃CO₂H/ CH₂Cl₂.

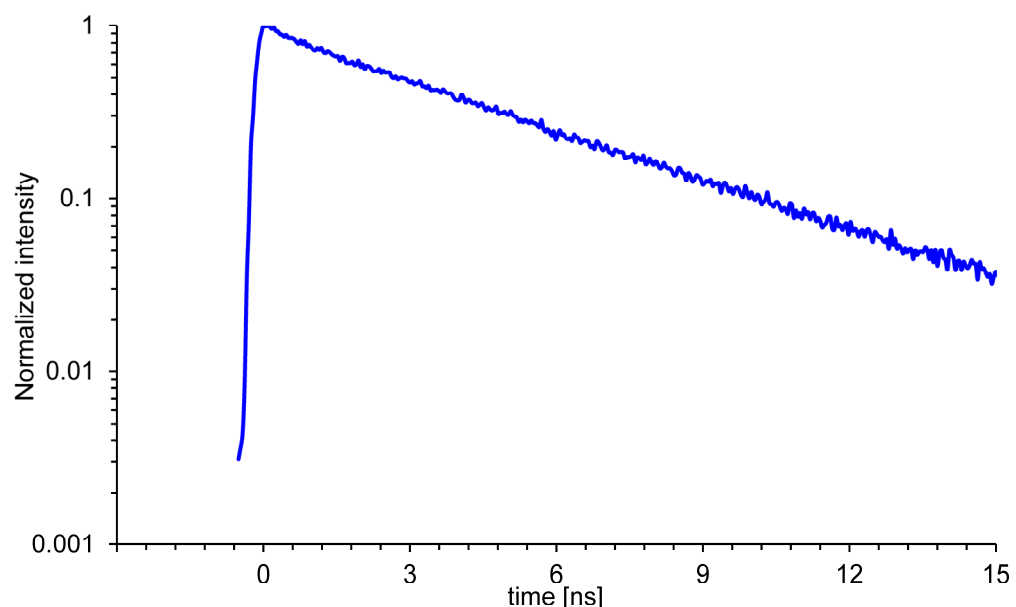


Figure S20. Fluorescence decay profile of **2b** in 10% CF₃CO₂H/ CH₂Cl₂.

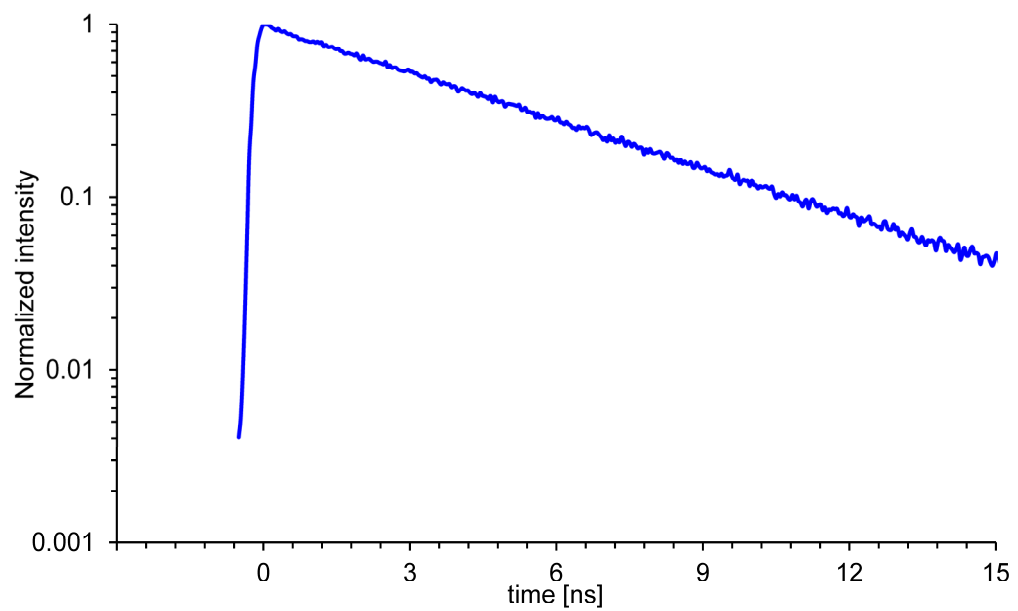
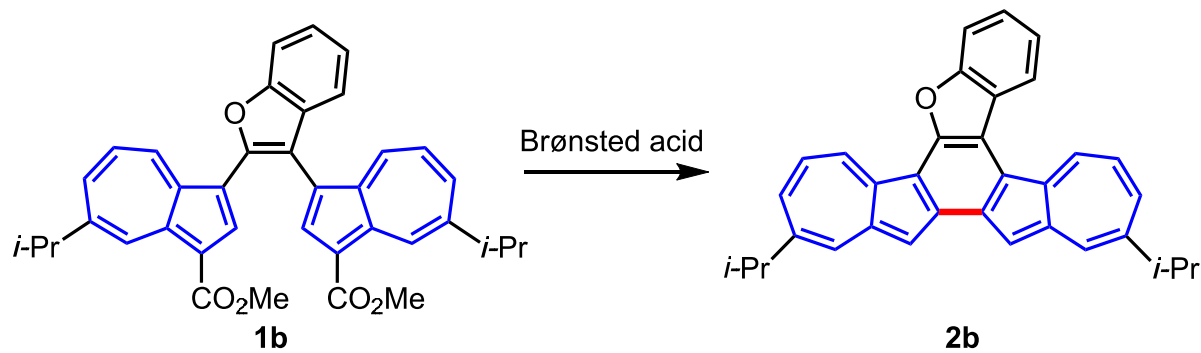


Figure S21. Fluorescence decay profile of **2c** in 10% $\text{CF}_3\text{CO}_2\text{H}/\text{CH}_2\text{Cl}_2$.

5. Scope and limitation

The annulation reaction of **1b** was chosen as a model compound for the optimizing the reaction conditions, using various Brønsted acids. As detailed in Table S2, the yields of the product were significantly dependent on the Brønsted acid employed. The annulation of **1b** in the presence of $\text{CH}_3\text{SO}_3\text{H}$ and $\text{CF}_3\text{SO}_3\text{H}$ resulted in the cyclized product **2b** with yields of 51% and 34%, respectively (entries 2 and 3). However, the annulation reaction did not occur in the presence of carboxylic acids, such as $\text{CH}_3\text{CO}_2\text{H}$ and $\text{CF}_3\text{CO}_2\text{H}$, resulting in the recovery of the starting material (entries 4 and 5). Among the tested Brønsted acids, 100% H_3PO_4 was found to provide the best product yield (entry 1).

Table S2. Optimization of the reaction conditions.

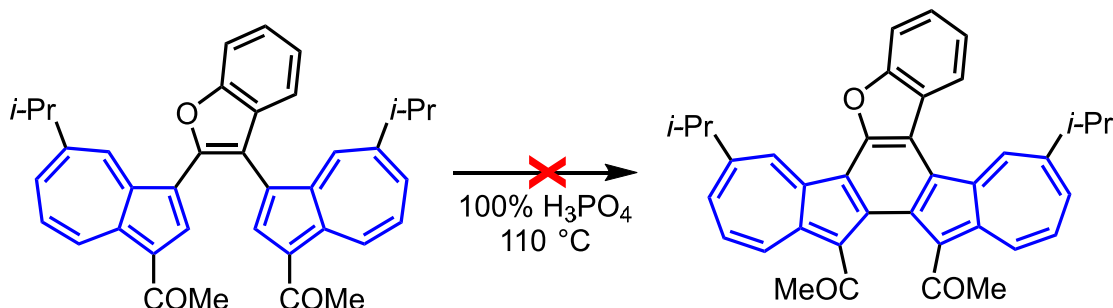


Entry	Brønsted acid	Yield [%]
1	100% H_3PO_4	77
2	$\text{CH}_3\text{SO}_3\text{H}$	51
3	$\text{CF}_3\text{SO}_3\text{H}^*$	34
4	$\text{CH}_3\text{CO}_2\text{H}$	No reaction
5	$\text{CF}_3\text{CO}_2\text{H}^*$	No reaction

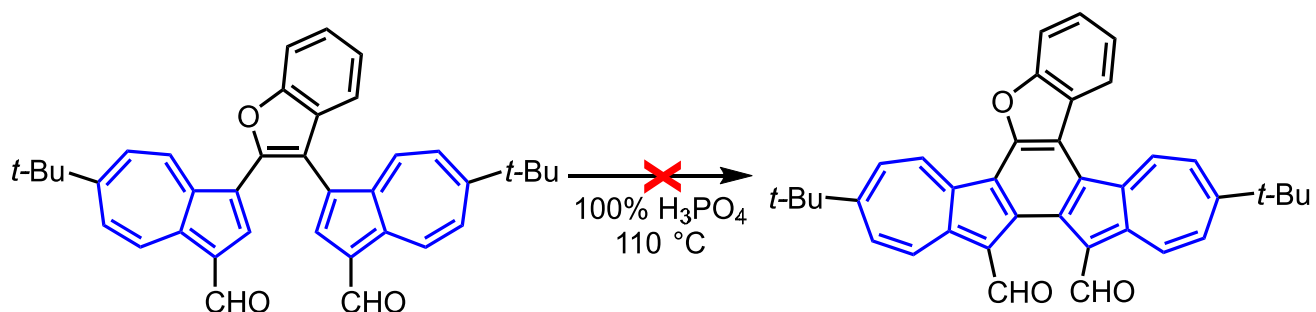
* refluxed in 1,2-dichloroethane.

The intramolecular cyclization of 2,3-di(3-acetyl- and 3-formyl-1-azulenyl)benzofurans was also investigated under the optimal conditions. However, in these reactions, neither the elimination of the substituent at the 3-position, i.e., acetyl and formyl groups, nor the cyclization reaction

proceeded resulting in the recovery of the starting materials, respectively. These results support the mechanism for the formation of **2a–2c** by the decarboxylation through the protonation of azulene rings followed by the intramolecular cyclization by the thermal 6π -electrocyclization as shown in Scheme 1.



Scheme S1. Attempt to the cyclization of 2,3-di(3-acetyl-7-isopropyl-1-azulenyl)benzofuran.



Scheme S2. Attempt to the cyclization of 2,3-di(3-formyl-6-*tert*-butyl-1-azulenyl)benzofuran.